Published in final edited form as:
Exp Brain Res. 2012 July ; 220(2): 121–133. doi:10.1007/s00221-012-3122-8.

Collateralization of Projections from the Rostral Ventrolateral Medulla to the Rostral and Caudal Thoracic Spinal Cord in Felines

Michael F. Gowen[1], **Sarah W. Ogburn**[2], **Takeshi Suzuki**[2], **Yoichiro Sugiyama**[2], **Lucy A. Cotter**[2], and **Bill J. Yates**[1,2]

[1]Department of Neuroscience, University of Pittsburgh, Pittsburgh, PA, USA 15213

[2]Department of Otolaryngology, University of Pittsburgh, Pittsburgh, PA, USA 15213

Abstract

Stimulation of vestibular receptors elicits distinct changes in blood flow to the forelimb and hindlimb, showing that the nervous system has the capacity to produce changes in sympathetic outflow that are specific for a particular region of the body. However, it is unclear whether the rostral ventrolateral medulla (RVLM), the primary region of the brainstem that regulates sympathetic outflow to vascular smooth muscle, has the appropriate connectivity with sympathetic preganglionic neurons to generate anatomically patterned responses. To make this determination, the retrograde fluorescent tracer Fast Blue was injected into the T_4 spinal cord segment of cats, which regulates upper body blood flow, whereas Fluoro-Ruby was injected into the T_{10} segment to label projections to a region of the spinal cord that regulates lower body blood flow. More neurons were single-labeled by a particular tracer (92%) than were double-labeled by both tracers (8%), supporting the notion that the RVLM can regulate sympathetic outflow from a limited number of spinal cord segments. Since a large fraction of RVLM neurons that control sympathetic outflow in rodents contain epinephrine, we additionally determined whether the tracer-labeled cells were immunopositive for the enzyme tyrosine hydroxylase (TH), which participates in the synthesis of catecholamines. Double-labeling by the two tracers injected into the spinal cord was more common for TH-immunopositive neurons than for the general population of RVLM neurons: 19% of the TH-positive cells contained both Fast Blue and Fluoro-Ruby, 30% contained one of the tracers, and 51% were not labeled by either tracer. Furthermore, many spinally-projecting neurons in close proximity to the RVLM catecholaminergic neurons (41% of the population) were not immunopositive for TH, suggesting that feline RVLM is neurochemically heterogeneous.

Keywords

Sympathetic nervous system; Blood pressure; Vascular resistance

Introduction

Walter Cannon first proposed that the sympathetic nervous system functions to elicit “fight or flight” responses, in which all sympathetic efferents are activated simultaneously (Cannon 1963). However, sympathetic preganglionic neurons have a topographic organization in the spinal cord. By injecting fluorescent tracers into different sympathetic

Address Correspondence To: Dr. Bill Yates, University of Pittsburgh, Department of Otolaryngology, Room 519, Eye and Ear Institute, Pittsburgh, PA 15213, Phone: 1-412-647-9614, FAX: 1-412-647-0108, byates@pitt.edu, URL: http://www.pitt.edu/~byates/yates.html.

prevertebral ganglia, Strack et al. (Strack et al. 1988) demonstrated that sympathetic preganglionic neurons in the upper thoracic cord regulate sympathetic outflow to the upper body, whereas sympathetic preganglionic neurons in the lower thoracic and upper lumbar spinal cord regulate sympathetic outflow to the lower body. In addition, transneuronal tracing studies that injected retrogradely-transported viruses into sympathetically-innervated targets in the hindlimb (Ugolini 1992; Lee et al. 2007) and tail (Smith et al. 1998) showed that all the sympathetic preganglionic neurons that regulate lower body smooth muscle are confined to the lower thoracic and upper lumbar spinal segments. Consequently, in order for global activation of sympathetic outflow to occur, brainstem presympathetic neurons must simultaneously activate sympathetic preganglionic neurons located throughout the length of the thoracic and upper lumbar spinal cord.

Recent studies have suggested that the brainstem has the capacity to independently control sympathetic outflow to different tissues, refuting Cannon's theories about the neural mechanisms that regulate sympathetic nervous system activity. Several of these studies focused on the primary region of the brainstem that regulates sympathetic outflow to vascular smooth muscle: the reticular formation of the rostral ventrolateral medulla (RVLM). Stimulation of the RVLM produced large increases in blood pressure and vasoconstriction in a variety of vascular beds (Dampney et al. 1982; Dampney et al. 1985; McAllen 1986a; McAllen 1986b; Dampney et al. 1987a; Dampney and McAllen 1988; McAllen and Dampney 1989; McAllen and Dampney 1990; McAllen et al. 1994), but in felines did not affect pupillary dilation, piloerection, gastrointestinal motility, or sweating, showing that this area does not globally activate sympathetic efferent fibers (McAllen 1986a). Furthermore, bilateral lesions of the RVLM induced a profound drop in blood pressure (Feldberg and Guertzenstein 1976; Dean and Coote 1986; Stein et al. 1989). Microinjections of the excitatory amino acid glutamate into the RVLM of cats produced decreases in blood flow to particular tissues (muscle, skin, or viscera) (Dampney and McAllen 1988; McAllen and Dampney 1990; Dean et al. 1992), although the particular tissue that showed reduced blood flow was affected throughout the body (Dampney and McAllen 1988; McAllen and Dampney 1990). For example, glutamate injections into the RVLM that caused increased muscle blood flow elicited similar changes in both forelimb and hindlimb perfusion (McAllen and Dampney 1990). Studies in humans also suggested that RVLM neurons have the capacity to regulate blood flow to particular tissues, but not particular body regions. For instance, mild unloading of cardiopulmonary afferents (Rea and Wallin 1989) or mental stress (Carter et al. 2005) resulted in an increase in the activity of muscle vasoconstrictor fibers in both the arms and legs.

Conversely, several studies in cats showed that vestibular stimulation evoked patterned changes in blood flow to different body regions. Electrical stimulation of vestibular afferents elicited distinct changes in the activity of muscle vasoconstrictor fibers in the upper and lower body (Kerman et al. 2000b), as well as opposite changes in forelimb and hindlimb blood flow (Kerman et al. 2000a). In addition, a bilateral labyrinthectomy abolished the increase in hindlimb vasoconstriction that ordinarily occurs during head-up tilts, but had no appreciable effect on forelimb blood flow (Wilson et al. 2006). Activation of the vestibulosympathetic reflex in humans by head-down neck flexion can also induce divergent changes in arm and leg blood flow during some phases of the menstrual cycle (Lawrence et al. 2010). Since vestibular influences on sympathetic outflow are mediated by RVLM neurons (Yates et al. 1995), these findings raise the possibility that individual RVLM neurons make connections with sympathetic preganglionic neurons in either the upper or lower thoracic spinal cord. This would allow for independent control of upper and lower body vasculatures. However, very little is known about the collateralization of the projections of RVLM neurons. One previous experiment demonstrated that a subset of RVLM neurons with a projection to the vicinity of the intermediolateral cell column in T3

could not be antidromically activated from more caudal spinal levels, showing that some RVLM cells selectively influence sympathetic preganglionic neurons in the upper thoracic spinal cord (Barman et al. 1985). Another study also showed that large injections of horseradish peroxidase into one spinal segment only labeled a subset of RVLM neurons (Polson et al. 1992). However, the propensity for RVLM neurons to make connections with sympathetic preganglionic neurons in particular spinal segments has not been thoroughly examined. In the present study, we injected two fluorescent tracers, Fast Blue and Fluoro-Ruby, into the T_4 and T_{10} spinal segments, respectively. We then determined the percentage of RVLM neurons that was labeled by only one or both of the tracers. Since a large fraction of the RVLM neurons that regulate sympathetic outflow in rodents contain epinephrine (Ruggiero et al. 1994; Madden and Sved 2003), we additionally determined whether the tracer-labeled cells were immunopositive for the enzyme tyrosine hydroxylase (TH), which participates in the synthesis of catecholamines (Cooper et al. 2003).

Methods and materials

Surgical procedures

Experiments were conducted on 6 male and 6 female purpose-bred cats weighing 2.7-4.8 Kg (median of 3.9 Kg), obtained from Liberty Research (Waverly, NY). All procedures on animals were approved by the University of Pittsburgh's Institutional Animal Care and Use Committee. An aseptic surgery was conducted in a dedicated operating room to inject the fluorescent tracers Fast Blue (Polysciences, Inc., Warrington, PA) and Fluoro-Ruby (Fluorochrome, LLC, Denver, CO) into the spinal cord. Animals were initially anesthetized by an intramuscular injection of ketamine (20 mg/kg) and acepromazine (0.2 mg/kg). Subsequently, an endotracheal tube and intravenous catheter were inserted. Anesthesia was supplemented as necessary by using 1-1.5% isoflurane vaporized in O_2 to maintain areflexia and a stable heart rate. Ringer lactate solution was infused intravenously to replace fluid loss during the surgery. A heating pad and heat lamp were used to maintain core temperature near 38°C.

Small laminectomies were performed to expose the T_4 and T_{10} spinal cord segments, although in two control experiments only one segment was exposed. The dura was opened, and a 0.5 μl Hamilton syringe maneuvered with a Narishige manipulator was used to make injections of 3% Fast Blue into the T_4 spinal cord or 5% Fluoro-Ruby into the T_{10} spinal cord. The needle of the syringe was inserted through the dorsal surface of the right spinal cord, just medial to the dorsal root entry zone, to a depth of approximately 2 mm. Three injections, spaced 1 mm apart in the rostral-caudal plane, were made in an attempt to label the descending projections from the brainstem to the intermediolateral cell column across the rostral-caudal extent of the injected segment. The volume of each injection is indicated in Table 1. Each injection was made slowly, over a 5-min period. Furthermore, we carefully observed the injection site using a surgical microscope to verify that no tracer escaped from the cord around the sides of the needle. Large injections were included in some experiments to minimize the potential of obtaining false negative results, by not distributing tracer thoroughly through the intermediolateral cell column in the target segments. However, in two control experiments (C101 and C102), the needle was inserted more laterally, through the dorsal root entry into the dorsolateral and lateral funiculi, where the axons of RVLM neurons are located in felines (Barman and Gebber 1985; Dampney et al. 1987b). These experiments were conducted to ascertain whether injections of tracers into the white matter would result in brainstem labeling through uptake by fibers of passage.

After the injections were completed, the muscle overlying the exposed spinal segments was closed. Following surgeries, animals received antibiotics (amoxicillin, two 50-mg oral doses

per day) for 10 days. For 72 h after the surgery, analgesia was provided through transdermal delivery of fentanyl (25 μg/h; Janssen Pharmaceutical Products, Titusville, NJ).

Animals recovered for two weeks following the injections, when they were anesthetized using ketamine (15 mg/kg) and acepromazine (1 mg/kg) injected intramuscularly, followed by pentobarbital sodium (40 mg/kg) injected intraperitoneally. After verifying the absence of nociceptive reflexes, the animals were transcardially perfused with 1 liter of heparinized saline followed by 2 liters of 4% paraformaldehyde-lysine-periodate fixative (McLean and Nakane 1974). The brain and spinal cord were removed, postfixed in 4°C paraformaldehyde-lysine-periodate, and cryoprotected in 30% sucrose in 0.1 M phosphate-buffered saline (PBS) for 2 days. Transverse spinal cord and brainstem sections were cut at a thickness of 40 μm using a freezing microtome, and collected as six sets.

To determine the locations of injection sites, sets of T_4 and T_{10} spinal cord sections were mounted serially, dehydrated with alcohol/xylenes, and coverslipped with DPX mounting media. Sections were observed using an Olympus BX51TRF photomicroscope equipped with a Hamamatsu camera (Hamamatsu Photonics, Hamamatsu, Japan) and a Simple-32 PCI image analysis system (Compix, Lake Oswego, OR) and photographed using a 4X objective. Montages of images were assembled using PTGui-Pro photostitching software (New House Internet Services BV, The Netherlands).

One bin of brainstem sections from each animal was also mounted serially and coverslipped as described above. The regions of the ventral medulla containing the RVLM and raphe pallidus and obscurus were photographed at low and high magnification. The medullary raphe nuclei were considered in the analysis, to determine whether the number of double-labeled cells observed in the RVLM was comparable to another brainstem area with spinal projections.

In an additional analysis, we determined whether the tracer-labeled RVLM neurons were immunopositive for TH. For this purpose, we made use of rabbit polyclonal anti-TH antibody (catalog # AB152, Millipore, Temecula, CA). To confirm the specificity of the antibody, one well of tissue was processed using avidin-biotin immunoperoxidase techniques (Hsu et al. 1981) to detect TH-containing neurons; a 1:1000 concentration of antibody was used in this analysis. Subsequently, the distribution of TH-immunopositive neurons in the brainstem was compared to that previously documented for the cat (Ruggiero et al. 1986; Jones and Beaudet 1987).

For the experiments where both the Fast Blue and Fluoro-Ruby injections produced labeling in the RVLM, an additional bin of tissue was processed using immunofluorescent techniques to identify neurons that contained TH. Tissue was incubated in anti-TH antibody at 1:500 concentration for 48 hrs, and then goat anti-rabbit fluorescent-tagged secondary antibody (DyLight 488, Thermo Scientific, Rockford, IL) at 1:500 concentration for 2 hrs. Afterwards, tissue was mounted and coverslipped using Vectashield HardSet Mounting Medium (Vector Laboratories, Burlingame, CA). Sections through the RVLM were photographed as described above and observed at high power to determine the fraction of neurons containing Fast Blue, Fluoro-Ruby, and both tracers that also expressed TH. During the analysis, we used illumination that independently elicited fluorescence of the Fast Blue and Fluoro-Ruby tracers, as well as the green DyLight 488 fluorophor that marked TH-immunopositive neurons, to assure that we accurately classified single-, double-, and triple-labeled cells.

Data were tabulated, and statistical analyses were performed, using Prism 5 software (GraphPad Software, San Diego, CA). Pooled data are represented as means ± one standard error.

Results

For the purpose of this study, the RVLM was defined as the region of the reticular formation spanning 1 mm from the ventral surface of the brainstem, lateral to the inferior olivary nucleus but medial to the spinal trigeminal nucleus, and from the rostral tip of the inferior olivary nucleus to 2 mm more caudally. The area of the reticular formation considered to constitute the RVLM is indicated in Fig. 1, and is based on a synthesis of previous anatomical and physiological descriptions of the area in the cat (Barman and Gebber 1983; Barman and Gebber 1985; Dampney et al. 1987a; Polson et al. 1992; Dampney 1994; Barman et al. 2011; DeStefino et al. 2011; Sugiyama et al. 2011), with a particular focus on the results of neurophysiological studies, which mapped the locations of RVLM neurons having activity synchronized to the cardiac cycle (Barman et al. 2011; DeStefino et al. 2011) or sympathetic nerve discharges (Barman and Gebber 1983; Barman and Gebber 1985). Substantial Fast Blue and Fluoro-Ruby labeling was present in the RVLM in six of the 12 animals: C10, C12, C13, C28, C48, and C51.

During histological processing of the spinal cord, sections through the sites that the needle penetrated typically became shredded, and thus these sections were lost. As such, to determine the region of the spinal cord where tracer was deposited, we observed sections adjacent to each injection site; Fig. 2 illustrates montages of photomicrographs showing tracer neighboring each of the three injection sites in the T_4 and T_{10} spinal cord of animal C12. Tracer was usually present throughout the region spanning between the injection sites. For some cases it was difficult to differentiate between the three separate injections, although a general representation of where the tracer was injected could be determined. Fig. 3 illustrates for every animal the area permeated by tracer. In one case (T_{10} segment of animal C47), tracer was clearly present in the tissue, but it was difficult to determine the precise areas that were infiltrated.

No labeled cell bodies were observed in the brainstem for the two control experiments (animals C101 and C102), where tracer was injected into the dorsolateral funiculus. RVLM cells in animal C11 were labeled by Fluoro-Ruby injected into T_{10}, but not Fast Blue injected into T_4. The Fast Blue injection sites in this case were large, but apparently confined to the dorsal horn and white matter. Animal C49 had Fast Blue labeling in the RVLM, but no Fluoro-Ruby labeling. In addition, RVLM labeling from both tracers was absent in cases C24 and C47. However, both Fluoro-Ruby and Fast Blue labeling was evident in other areas of the brainstem, including the medullary raphe nuclei, for three cases where cells in the RVLM were unlabeled by one or both of the tracers (C11, C47, and C49), showing that the tracers were effectively transported to the brainstem. A commonality of most of the cases where cells in the RVLM did not contain either Fast Blue or Fluoro-Ruby (Fast Blue in animals C11 and C101; Fluoro-Ruby in animals C49 and C102) is limited inclusion of the intermediolateral cell column in the injected area.

Fig. 4 shows the locations of RVLM neurons labeled by Fast Blue and Fluoro-Ruby in sections from animal C48. Photomicrographs of tracer-labeled neurons from this animal are provided in Fig. 5A. The labeled cells in the RVLM were small to medium in size, and could be easily distinguished from the larger neurons located more dorsally in the reticular formation. Approximately nine sections (minimum of eight) from each animal spanning from the rostral tip of the inferior olivary nucleus to approximately 2 mm more caudally were selected for quantification of labeling in the RVLM. Counts and measurements of the locations of labeled RVLM neurons relative to the rostral tip of the inferior olivary nucleus, the ventral surface of the brainstem, and the midline were generated from photomontages of the ventral portion of the rostral medulla in combination with high-magnification micrographs and observations through the microscope. Care was taken to distinguish

between double-labeled cells that contained both Fluoro-Ruby and Fast Blue, and overlapping cells that each contained one of the fluorophors. The average locations of labeled neurons are provided in Table 2.

Of the 680 RVLM neurons labeled by tracer injections into the spinal cord, 304 (41%) were on the left (contralateral) side, and 434 (59%) were on the right (ipsilateral) side. Fig. 6A shows for each animal the average number of RVLM neurons observed per section that were labeled by Fast Blue, Fluoro-Ruby, or both tracers. The number of double-labeled cells in any experiment was very low (average of 1.0 ± 0.2 neurons/section). On average across experiments, only 8.2±1.2% of the RVLM cells that contained tracer were double-labeled. To provide a comparison, for each animal we also counted the number of labeled cells in raphe pallidus and obscurus in ~8 sections through the rostral medulla. Fig. 6B indicates the average number of labeled cells/section observed in the raphe nuclei. Both the total number of labeled cells per section as well as the number of double-labeled cells was higher in the raphe nuclei than in the RVLM. Fig. 6C compares the total number of labeled cells and the number of double-labeled cells/section in the two regions. Values are shown as the number of cells per section in the RVLM as a fraction of the number of cells per section in the raphe nuclei. The right column of Fig. 6C indicates the average of the values obtained for each animal. Whereas the RVLM contained 25.3% of the total number of labeled cells per section as did the raphe nuclei, RVLM double labeling was only 7.6% of raphe double labeling. These two quantities were shown to be significantly different through a Mann-Whitney test ($p=0.03$), indicating that the differences in double labeling between the raphe nuclei and RVLM was not simply related to the higher amount of total raphe labeling.

Since over 50% of spinally-projecting RVLM neurons that regulate sympathetic outflow in rodents synthesize epinephrine (Ruggiero et al. 1994; Madden and Sved 2003), we additionally determined whether the neurons labeled by injections of Fast Blue and Fluoro-Ruby into the spinal cord were immunopositive for TH. By observing brainstem sections processed using immunoperoxidase techniques, we confirmed that the TH-immunopositive neurons were confined to regions known to contain catecholaminergic neurons, including the following areas: nucleus tractus solitarius, the rostral ventrolateral medulla, the caudal medullary lateral tegmental field near the lateral reticular nucleus, the pontine lateral tegmental field surrounding the superior olivary nucleus, and nucleus coeruleus (Ruggiero et al. 1986; Jones and Beaudet 1987). Micrographs of immunoperoxidase-stained TH neurons in the RVLM and nucleus tractus solitarius are provided in Figs. 7A and 7B, respectively. The catecholaminergic RVLM neurons comprised an “L-shaped” area, which included a column spanning ventrally from the retrofacial nucleus to the surface that continued ~1 mm medially along the ventral aspect of the brainstem (see Fig. 7A).

Counts were obtained of the number of tracer-labeled and TH-immunopositive neurons present within the cluster of catecholaminergic neurons in the RVLM. Fig. 8 shows for each animal the average number of cells per section in this restricted region of the RVLM, as well as the averages for all animals. Micrographs showing combined immunofluorescence for tracers and TH are provided in Fig. 5B. Amongst the TH-immunopositive RVLM neurons, 51% contained no tracer, 17% contained only Fast Blue, 12% contained only Fluoro-Ruby, and 19% contained both tracers. However, 41% of the tracer-labeled cells clustered with the catecholaminergic neurons did not express TH. Of these non-TH cells, 95% were single-labeled by either Fast Blue or Fluoro-Ruby, and only 5% were double-labeled. The differences in double-labeling between TH-positive and TH-negative neurons clustered together in the RVLM were shown to be significant using a Mann-Whitney test ($p<0.03$).

Discussion

The major finding of this study is that only a small fraction (<10%) of RVLM neurons was double-labeled by injections of different fluorescent tracers into the T_4 and T_{10} spinal cord segments. However, double labeling was higher for catecholaminergic RVLM neurons (19% of the entire population and 41% of the tracer-labeled TH-immunopositve cells). In contrast, the large majority (95%) of non-catecholaminergic cells clustered with the TH-immunopositive neurons were selectively labeled by either Fast Blue or Fluoro-Ruby. These data suggest that some RVLM neurons in felines, particularly non-catecholaminergic neurons, can selectively control sympathetic outflow from particular spinal cord segments.

In rats, T_4 sympathetic preganglionic neurons were labeled by the injection of Fluoro-gold into the superior, middle and inferior cervical sympathetic ganglia (Strack et al. 1988), which innervate structures in the upper body (Lichtman et al. 1979). In contrast, T_{10} sympathetic preganglionic neurons were labeled by injection of Fluoro-gold into the celiac and mesenteric sympathetic ganglia (Strack et al. 1988), which innervate targets in the lower part of the body (Kerman et al. 2000c). Furthermore, T_{10}, but not T_4, sympathetic preganglionic neurons were transneuronally infected by the injection of neurotropic viruses into hindlimb muscles (Lee et al. 2007) or nerves (Ugolini 1992). Since the major function of RVLM neurons in the cat appears to be regulation of the activity of vasoconstrictor fibers (Dampney et al. 1982; Dampney et al. 1985; McAllen 1986a; McAllen 1986b; Dampney et al. 1987a; Dampney and McAllen 1988; McAllen and Dampney 1989; McAllen and Dampney 1990; McAllen et al. 1994), and not sympathetic efferents with functions other than cardiovascular regulation (McAllen 1986a), these findings are consistent with the hypothesis that some RVLM neurons can independently regulate blood flow to the upper and lower body.

Studies showing that microinjections of excitatory amino acids into the RVLM of the cat produce reductions in blood flow to particular tissues (Dampney and McAllen 1988; McAllen and Dampney 1990; Dean et al. 1992), but the changes were similar in the upper and lower body (Dampney and McAllen 1988; McAllen and Dampney 1990), led to the notion that the RVLM cannot elicit anatomically-patterned alterations in vascular resistance. In the present study, neurons that were labeled by the injection of fluorescent tracers into the T_4 and T_{10} spinal cord were intermingled in the RVLM. Consequently, neurons projecting to both T_4 and T_{10} would be activated by stimulation of a particular RVLM region, resulting in similar changes in blood flow across the body axis. While resolving the apparent discrepancy between the results of experiments that stimulated particular areas of the RVLM (Dampney and McAllen 1988; McAllen and Dampney 1990) and studies showing that vestibular stimulation produces anatomically-patterned vascular responses (Kerman et al. 2000a; Kerman et al. 2000b; Wilson et al. 2006; Lawrence et al. 2010), these observations raise the question of how inputs to the RVLM can evoke such patterned effects. One possibility is that anatomically-patterned responses are the result of distinct inputs to adjacent RVLM neurons projecting to different levels of the spinal cord. Another possibility is that anatomical patterning is a consequence of the integrated inputs a neuron receives from multiple sources. Additional experiments must be conducted to address how the RVLM elicits distinct patterns of sympathetic outflow to different body regions.

Several caveats must be considered when interpreting the present findings. One concern is that the tracer injections did not label a large proportion of RVLM neurons projecting to a particular spinal cord segment. We minimized the risk of false negative results by making three tracer injections per cord segment, spaced 1 mm apart in the rostral-caudal plane. In over half the animals, the volume of each injection was very large (≥ 250 μl), and tracer was evident throughout the area spanning between the injection sites, as well as rostral and

caudal to the injection sites. In animals where RVLM neurons were labeled, the intermediolateral region of the spinal gray matter was thoroughly infiltrated with tracer (see Fig. 3). Furthermore, the injections typically produced substantial labeling in numerous areas of the brainstem, including the medullary raphe nuclei, which despite having a small area contained approximately four times the number of labeled cells per section as did the RVLM. Many raphe neurons were labeled by both Fast Blue and Fluoro-Ruby, demonstrating that we could effectively detect double-labeled cells. These findings provide assurance that the limited labeling in the RVLM was not due to inadequate uptake of tracer by bulbospinal neurons projecting to the target segments.

A second potential concern was that labeling of brainstem neurons was due to uptake of tracer by fibers of passage in the white matter, and not axonal terminals in the spinal gray matter. We addressed this concern by showing that tracer injections confined to the white matter did not produce any brainstem labeling (e.g., cases C101 and C102). Furthermore, no labeled cell bodies were detected in the RVLM unless the tracer injections impinged on the intermediolateral cell column. In addition, uptake of Fast Blue tracer in T_4 by fibers of passage would have resulted in appreciable double-labeling of RVLM neurons, and not the limited double labeling that we observed.

Another limitation in interpreting the present results is variations in the literature regarding the description of the region of the rostral medulla containing presympathetic neurons in cats. Most studies of the RVLM were conducted in rats, and the vast majority of cells classified as spinally-projecting RVLM neurons in this study were located in an area analogous to the rat RVLM (Card et al. 2006; Bourassa et al. 2009; Goodchild and Moon 2009; Holstein et al. 2011). Dampney suggested that the RVLM in the cat is much narrower than in the rat, and is comprised of a 0.2-0.5 mm wide column of cells beneath the retrofacial nucleus (Dampney 1994). This definition is at least partly based on a previous study where horseradish peroxidase was injected into the T_3 segment, which reported that virtually all of the spinally-projecting cells near the ventral surface of the RVLM were bundled in a tight column ventral to the retrofacial nucleus (Polson et al. 1992). In contrast, the neurons near the ventral surface of the rostral medulla labeled by tracer injections into T_4 and T_{10}, including those shown to express TH, were dispersed over a larger medial-lateral area. In addition, the locations of tracer-labeled cells near the ventral surface of the rostral medulla in this study correspond to those of neurons identified in neurophysiological studies as having activity synchronized to the cardiac cycle (Barman et al. 2011; DeStefino et al. 2011) or sympathetic nerve discharges (Barman and Gebber 1983; Barman and Gebber 1985). These findings suggest that bulbospinal RVLM neurons that participate in cardiovascular regulation have similar locations in rats and cats, and that the feline RVLM is likely larger than described in some studies (Dampney 1994).

Studies in rodents have demonstrated that at least half of the presympathetic neurons in the RVLM are catecholaminergic, and synthesize epinephrine (Ruggiero et al. 1994; Madden and Sved 2003). However, the present results suggest that the feline RVLM extends beyond the cluster of catecholaminergic neurons, and that many non-catecholaminergic neurons are interspersed between the TH-immunopositive cells. As such, it seems likely that less than 50% of RVLM neurons in felines that regulate sympathetic outflow are catecholaminergic. Studies in rats have suggested that a region of the rostral medulla located dorsal and lateral to the pyramids contains neurons that project to sympathetic preganglionic neurons (Schramm et al. 1993; Kerman et al. 2003; Lee et al. 2007); this region is typically referred to as the rostral ventromedial medulla (RVMM). Neurons in the RVMM participate in cardiovascular regulation (Cox and Brody 1989; Varner et al. 1992; Varner et al. 1994). In felines, the analogous area to the RVMM contains large spinally-projecting neurons that take part in motor control (Peterson et al. 1975). One possibility is that the RVMM is

displaced laterally in felines and merges with the RVLM, to form a single, neurochemically heterogeneous area that regulates sympathetic outflow. One piece of evidence that supports this view is the relative location in rats and cats of serotoninergic neurons along the ventral surface of the rostral medulla. In rodents, these serotoninergic neurons are located in the RVMM, which form a lateral extension of the raphe nuclei (Tanaka et al. 1994; Huang and Weiss 1999; Kerman et al. 2006). This lateral extension of the raphe nuclei is absent in cats, but a large population of serotoninergic neurons is concentrated more laterally in the area defined as the RVLM in this study (Rice et al. 2009). Additional studies are needed to determine if serotoninergic RVLM neurons participate in cardiovascular regulation in felines. A lateral column of serotonergic neurons is also present in the RVLM of humans (Hornung 2003), apparently overlapping the catecholaminergic neurons in this region (Benarroch et al. 1998). These findings raise the possibility that the human RVLM, like that in the feline, is neurochemically heterogeneous.

In summary, the results of this study support the notion that subsets of RVLM neurons project to the upper and lower thoracic spinal cord in cats, raising the possibility that the area can elicit regionally-specific changes in blood flow. In particular, non-catecholaminergic RVLM neurons were more likely to be selectively labeled by injections of different fluorescent tracers into T_4 and T_{10}. However, this conclusion does not preclude the possibility that additional brainstem regions that project to sympathetic preganglionic neurons also contribute to producing alterations in blood flow limited to a particular body region. For example, there is some evidence that neurons outside of the RVLM, perhaps in the medullary raphe nuclei, participate in the anatomical patterning of vestibulo-sympathetic reflexes (Sugiyama et al. 2011). In addition, the present findings raise the possibility that the RVLM is more neurochemically heterogeneous in cats than in rodents. It is feasible that some of the spinally-projecting, non-catecholaminergic RVLM neurons in felines were serotoninergic, because many serotonin-synthesizing neurons are present in this region in cats but not rodents (Rice et al. 2009). These species differences suggest that additional comparative studies should be conducted, including experiments in nonhuman primates, to determine how the organization of the RVLM differs between mammals.

Acknowledgments

The authors thank Vincent DeStefino and Laura Carlino for technical assistance. Funding was provided by Grant R01-DC00693 from the National Institutes of Health (USA). Michael Gowen was supported by an American Physiological Society Undergraduate Summer Research Fellowship.

References

Barman SM, Gebber GL. Sequence of activation of ventrolateral and dorsal medullary sympathetic neurons. Am J Physiol. 1983; 245:R438–447. [PubMed: 6614214]

Barman SM, Gebber GL. Axonal projection patterns of ventrolateral medullospinal sympathoexcitatory neurons. J Neurophysiol. 1985; 53:1551–1566. [PubMed: 2989448]

Barman SM, Sugiyama Y, Suzuki T, Cotter LA, DeStefino VJ, Reighard DA, Cass SP, Yates BJ. Rhythmic activity of neurons in the rostral ventrolateral medulla of conscious cats: effect of removal of vestibular inputs. Am J Physiol Regul Integr Comp Physiol. 2011; 301:R937–946. [PubMed: 21734018]

Benarroch EE, Smithson IL, Low PA, Parisi JE. Depletion of catecholaminergic neurons of the rostral ventrolateral medulla in multiple systems atrophy with autonomic failure. Ann Neurol. 1998; 43:156–163. [PubMed: 9485056]

Berman, AI. The Brain Stem of the Cat. University of Wisconsin Press; Madison: 1968.

Bourassa EA, Sved AF, Speth RC. Angiotensin modulation of rostral ventrolateral medulla (RVLM) in cardiovascular regulation. Molec Cell Endocrinol. 2009; 302:167–175. [PubMed: 19027823]

Cannon, WB. The Wisdom of the Body. W. W. Norton; New York: 1963.

Card JP, Sved JC, Craig B, Raizada M, Vazquez J, Sved AF. Efferent projections of rat rostroventrolateral medulla C1 catecholamine neurons: Implications for the central control of cardiovascular regulation. J Comp Neurol. 2006; 499:840–859. [PubMed: 17048222]

Carter JR, Kupiers NT, Ray CA. Neurovascular responses to mental stress. J Physiol. 2005; 564:321–327. [PubMed: 15705649]

Cooper, JR.; Bloom, FE.; Roth, RH. The Biochemical Basis of Neuropharmacology. Oxford University Press; New York: 2003.

Cox BF, Brody MJ. Subregions of rostral ventral medulla control arterial pressure and regional hemodynamics. Am J Physiol. 1989; 257:R635–640. [PubMed: 2782466]

Dampney RA. The subretrofacial vasomotor nucleus - anatomical, chemical and pharmacological properties and role in cardiovascular regulation. Prog Neurobiol. 1994; 42:197–227. [PubMed: 8008825]

Dampney RA, Goodchild AK, McAllen RM. Vasomotor control by subretrofacial neurones in the rostral ventrolateral medulla. Can J Physiol Pharmacol. 1987a; 65:1572–1579. [PubMed: 3319108]

Dampney RA, Goodchild AK, Robertson LG, Montgomery W. Role of ventrolateral medulla in vasomotor regulation: a correlative anatomical and physiological study. Brain Res. 1982; 249:223–235. [PubMed: 6128058]

Dampney RAL, Czachurski J, Dembowsky K, Goodchild AK, Seller H. Afferent connections and spinal projections of the pressor region in the rostral ventrolateral medulla of the cat. J Autonom Nerv Syst. 1987b; 20:73–86.

Dampney RAL, Goodchild AK, Tan E. Vasopressor neurons in the rostral ventrolateral medulla of the rabbit. J Autonom Nerv Syst. 1985; 14:239–254.

Dampney RAL, McAllen RM. Differential control of sympathetic fibres supplying hindlimb skin and muscle by subretrofacial neurones in the cat. J Physiol. 1988; 395:41–56. [PubMed: 2900889]

Dean C, Coote JH. A ventromedullary relay involved in the hypothalamic and chemoreceptor activation of sympathetic postganglionic neurones to skeletal muscle, kidney and splanchnic area. Brain Res. 1986; 377:279–285. [PubMed: 3730863]

Dean C, Seagard JL, Hopp FA, Kampine JP. Differential control of sympathetic activity to kidney and skeletal muscle by ventral medullary neurons. J Autonom Nerv Syst. 1992; 37:1–10.

DeStefino VJ, Reighard DA, Sugiyama Y, Suzuki T, Cotter LA, Larson MG, Gandhi NJ, Barman SM, Yates BJ. Responses of neurons in the rostral ventrolateral medulla (RVLM) to whole-body rotations: comparisons in decerebrate and conscious cats. J Appl Physiol. 2011; 110:1699–1707. [PubMed: 21493724]

Feldberg W, Guertzenstein PG. Vasopressor effects obtained by drugs acting on the ventral surface of the brain stem. J Physiol. 1976; 258:337–355. [PubMed: 957160]

Goodchild AK, Moon EA. Maps of cardiovascular and respiratory regions of rat ventral medulla: Focus on the caudal medulla. J Chem Neuroanat. 2009; 38:209–221. [PubMed: 19549567]

Holstein GR, Friedrich VL Jr. Kang T, Kukielka E, Martinelli GP. Direct projections from the caudal vestibular nuclei to the ventrolateral medulla in the rat. Neurosci. 2011; 175:104–117.

Hornung JP. The human raphe nuclei and the serotonergic system. J Chem Neuroanat. 2003; 26:331–343. [PubMed: 14729135]

Hsu SM, Raine L, Fanger H. Use of avidin-biotin-peroxidase complex (ABC) in immunoperoxidase techniques: a comparison between ABC and unlabeled antibody (PAP) procedures. J Histochem Cytochem. 1981; 29:577–580. [PubMed: 6166661]

Huang J, Weiss ML. Characterization of the central cell groups regulating the kidney in the rat. Brain Res. 1999; 845:77–91. [PubMed: 10529446]

Jones BE, Beaudet A. Distribution of acetylcholine and catecholamine neurons in the cat brainstem: a choline acetyltransferase and tyrosine hydroxylase immunohistochemical study. J Comp Neurol. 1987; 261:15–32. [PubMed: 2887593]

Kerman IA, Emanuel BA, Yates BJ. Vestibular stimulation leads to distinct hemodynamic patterning. Am J Physiol Regul Integr Comp Physiol. 2000a; 279:R118–125. [PubMed: 10896872]

Kerman IA, Enquist LW, Watson SJ, Yates BJ. Brainstem substrates of sympatho-motor circuitry identified using trans-synaptic tracing with pseudorabies virus recombinants. J Neurosci. 2003; 23:4657–4666. [PubMed: 12805305]

Kerman IA, McAllen RM, Yates BJ. Patterning of sympathetic nerve activity in response to vestibular stimulation. Brain Res Bul. 2000b; 53:11–16.

Kerman IA, Shabrang C, Taylor L, Akil H, Watson SJ. Relationship of presympathetic-premotor neurons to the serotonergic transmitter system in the rat brainstem. J Comp Neurol. 2006; 499:882–896. [PubMed: 17072838]

Kerman IA, Yates BJ, McAllen RM. Anatomic patterning in the expression of vestibulosympathetic reflexes. Am J Physiol Regul Integr Comp Physiol. 2000c; 279:R109–117. [PubMed: 10896871]

Lawrence JE, Klein JC, Carter JR. Menstrual cycle elicits divergent forearm vascular responses to vestibular activation in humans. Auton Neurosci. 2010; 154:89–93. [PubMed: 19939746]

Lee TK, Lois JH, Troupe JH, Wilson TD, Yates BJ. Transneuronal tracing of neural pathways that regulate hindlimb muscle blood flow. Am J Physiol Regul Integr Comp Physiol. 2007; 292:R1532–1541. [PubMed: 17158263]

Lichtman JW, Purves D, Yip JW. On the purpose of selective innervation of guinea-pig superior cervical ganglion cells. J Physiol. 1979; 292:69–84. [PubMed: 490406]

Madden CJ, Sved AF. Rostral ventrolateral medulla C1 neurons and cardiovascular regulation. Cell Molec Neurobiol. 2003; 23:739–749. [PubMed: 14514028]

McAllen RM. Action and specificity of ventral medullary vasopressor neurones in the cat. Neurosci. 1986a; 18:51–59.

McAllen RM. Identification and properties of sub-retrofacial bulbospinal neurones: a descending cardiovascular pathway in the cat. J Auton Nerv Syst. 1986b; 17:151–164. [PubMed: 3782723]

McAllen RM, Dampney RA. The selectivity of descending vasomotor control by subretrofacial neurons. Prog Brain Res. 1989; 81:233–242. [PubMed: 2694221]

McAllen RM, Dampney RAL. Vasomotor neurons in the rostral ventrolateral medulla are organized topographically with respect to type of vascular bed but not body region. Neurosci Lett. 1990; 110:91–96. [PubMed: 1970144]

McAllen RM, Habler HJ, Michaelis M, Peters O, Janig W. Monosynaptic excitation of preganglionic vasomotor neurons by subretrofacial neurons of the rostral ventrolateral medulla. Brain Res. 1994; 634:227–234. [PubMed: 8131072]

McLean IW, Nakane PK. Periodate-lysine-paraformaldehyde for immunoelectron microscopy. J Histochem Cytochem. 1974; 22:1077–1083. [PubMed: 4374474]

Peterson BW, Maunz RA, Pitts NG, Mackel RG. Patterns of projections and branching of reticulospinal neurons. Exp Brain Res. 1975; 23:333–351. [PubMed: 1183508]

Polson JW, Halliday GM, McAllen RM, Coleman MJ, Dampney RA. Rostrocaudal differences in morphology and neurotransmitter content of cells in the subretrofacial vasomotor nucleus. J Auton Nerv Syst. 1992; 38:117–137. [PubMed: 1377728]

Rea RF, Wallin BG. Sympathetic nerve activity in arm and leg muscles during lower body negative pressure in humans. J Appl Physiol. 1989; 66:2778–2781. [PubMed: 2745341]

Rice CD, Lois JH, Kerman IA, Yates BJ. Localization of serotoninergic neurons that participate in regulating diaphragm activity in the cat. Brain Res. 2009; 1279:71–81. [PubMed: 19433074]

Ruggiero DA, Cravo SL, Golanov E, Gomez R, Anwar M, Reis DJ. Adrenergic and non-adrenergic spinal projections of a cardiovascular-active presser area of medulla oblongata: quantitative topographic analysis. Brain Res. 1994; 663:107–120. [PubMed: 7531595]

Ruggiero DA, Gatti PJ, Gillis RA, Norman WP, Anwar M, Reis DJ. Adrenaline-synthesizing neurons in the medulla of the cat. J Comp Neurol. 1986; 252:532–542. [PubMed: 3537023]

Schramm LP, Strack AM, Platt KB, Loewy AD. Peripheral and central pathways regulating the kidney - a study using pseudorabies virus. Brain Res. 1993; 616:251–262. [PubMed: 7689411]

Smith JE, Jansen AS, Gilbey MP, Loewy AD. CNS cell groups projecting to sympathetic outflow of tail artery: neural circuits involved in heat loss in the rat. Brain Res. 1998; 786:153–164. [PubMed: 9554992]

Stein RD, Weaver LC, Yardley CP. Ventrolateral medullary neurones: effects on magnitude and rhythm of discharge of mesenteric and renal nerves in cats. J Physiol. 1989; 408:571–586. [PubMed: 2778740]

Strack AM, Sawyer WB, Marubio LM, Loewy AD. Spinal origin of sympathetic preganglionic neurons in the rat. Brain Res. 1988; 455:187–191. [PubMed: 3416186]

Sugiyama Y, Suzuki T, Yates BJ. Role of the rostral ventrolateral medulla (RVLM) in the patterning of vestibular system influences on sympathetic nervous system outflow to the upper and lower body. Exp Brain Res. 2011; 210:515–527. [PubMed: 21267550]

Tanaka M, Okamura H, Tamada Y, Nagatsu I, Tanaka Y, Ibata Y. Catecholaminergic input to spinally projecting serotonin neurons in the rostral ventromedial medulla oblongata of the rat. Brain Res Bul. 1994; 35:23–30.

Ugolini G. Transneuronal transfer of herpes simplex virus type 1 (HSV 1) from mixed limb nerves to the CNS. I. Sequence of transfer from sensory, motor, and sympathetic nerve fibres to the spinal cord. J Comp Neurol. 1992; 326:527–548. [PubMed: 1336502]

Varner KJ, Rutherford DS, Vasquez EC, Brody MJ. Identification of cardiovascular neurons in the rostral ventromedial medulla in anesthetized rats. Hypertension. 1992; 19(2 Suppl):II, 193–197.

Varner KJ, Vasquez EC, Brody MJ. Lesions in rostral ventromedial or rostral ventrolateral medulla block neurogenic hypertension. Hypertension. 1994; 24:91–96. [PubMed: 8021014]

Wilson TD, Cotter LA, Draper JA, Misra SP, Rice CD, Cass SP, Yates BJ. Vestibular inputs elicit patterned changes in limb blood flow in conscious cats. J Physiol. 2006; 575:671–684. [PubMed: 16809368]

Yates BJ, Siniaia MS, Miller AD. Descending pathways necessary for vestibular influences on sympathetic and inspiratory outflow. Am J Physiol. 1995; 268:R1381–R1385. [PubMed: 7611512]

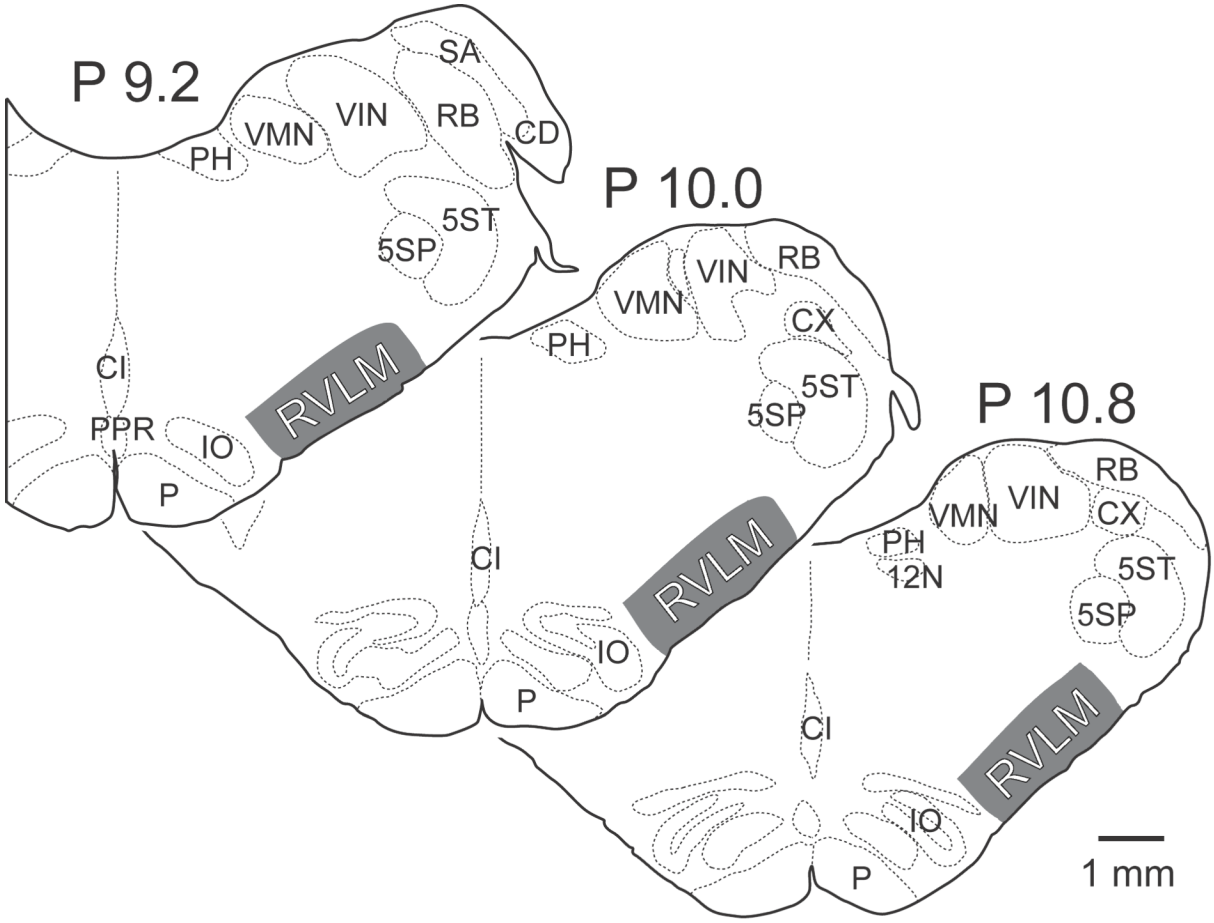

Figure 1.

Area of the brainstem that was considered to comprise the RVLM in this study. Numbers above each section indicate the level posterior *(P)* to stereotaxic zero, in accordance with Berman's atlas (Berman 1968). 5SP, spinal trigeminal nucleus; 5ST, spinal trigeminal tract; 12N, hypoglossal nerve; CD, dorsal cochlear nucleus; CI, inferior central nucleus; CX, external cuneate nucleus; IO, inferior olive; P, pyramid; PH, nucleus prepositus hypoglossi; PPR, postpyramidal nucleus of the raphe; RB, restiform body; SA, stria acustica; VIN, inferior vestibular nucleus; VMN, medial vestibular nucleus.

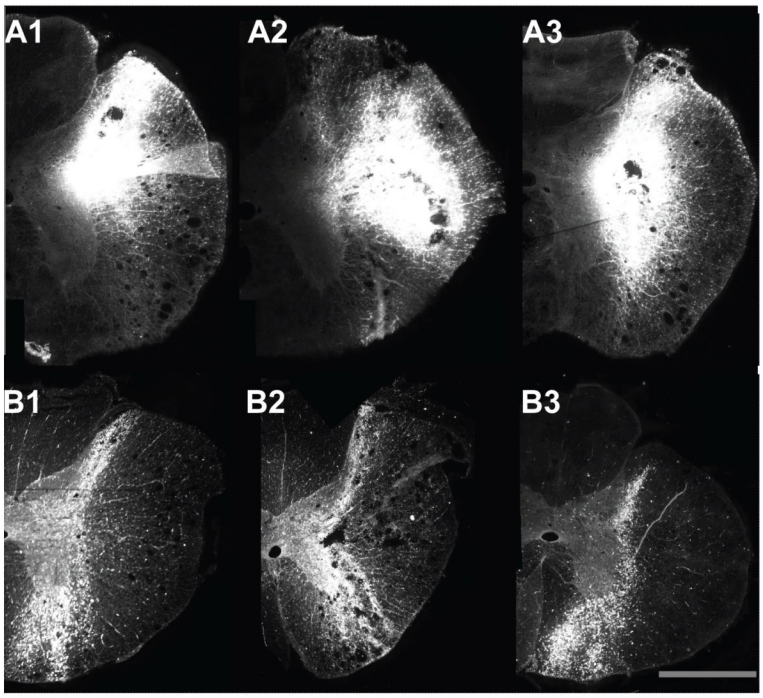

Figure 2.

Montages of photomicrographs showing injection sites in animal C12. ***A1-A3:*** the three injection sites observed in the T_4 segment. ***B1-B3:*** the three injection sites observed in the T_{10} segment. The calibration bar represents 1 mm.

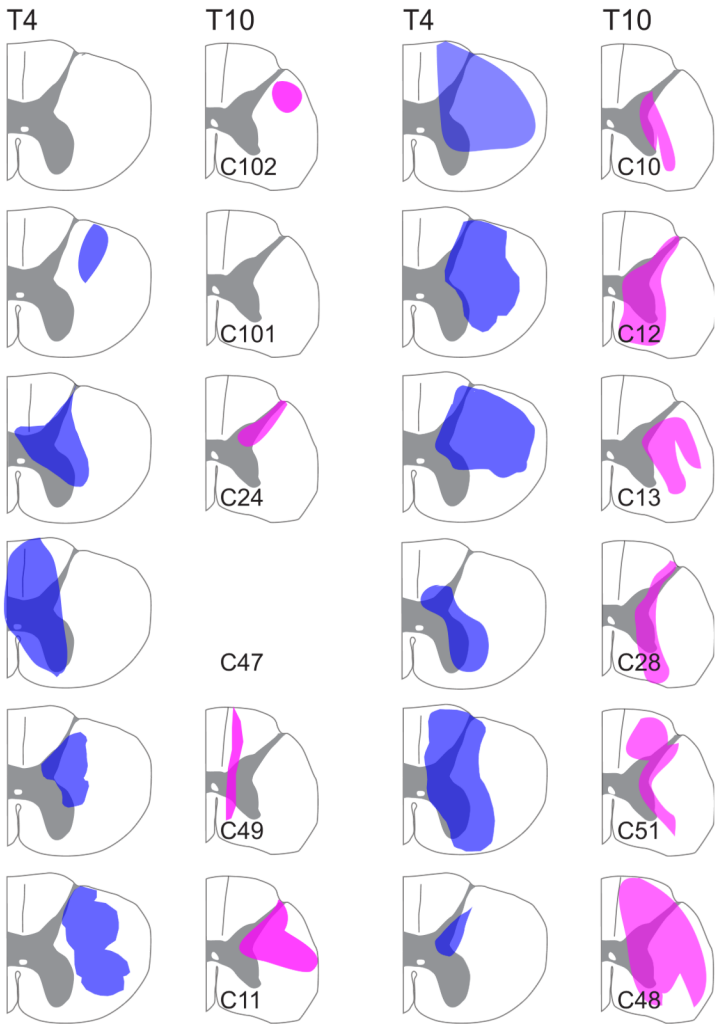

Figure 3.

The area of the spinal cord permeated by tracers in each animal. These drawings reflect the cumulative area where a tracer was observed in sections neighboring the injection sites. In sections where no injection sites are indicated on a drawing (animals C102 and C101), injections were only made in one segment. For one injection site (T10 segment of animal C47), although tracer was clearly present in the tissue, it was difficult to determine the precise areas that were infiltrated. This injection site was thus omitted.

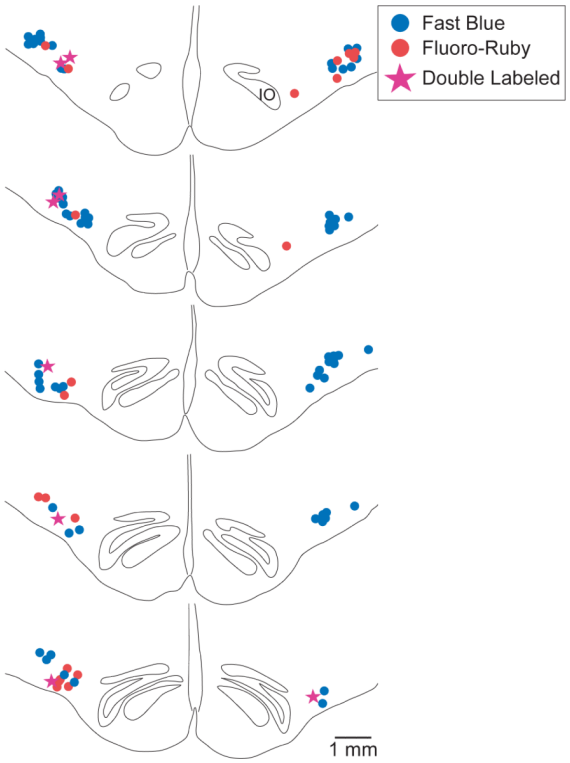

Figure 4.
A series of drawings of the ventral medulla of animal C48 showing the locations of RVLM neurons labeled by Fast Blue, Fluoro-Ruby, or both tracers. Drawings were constructed from montages of photomicrographs, which were used to determine the positions of labeled cells. The top section was located ~0.5 mm caudal to the rostral pole of the inferior olivary nucleus (IO); the sections below are spaced ~0.25 mm apart.

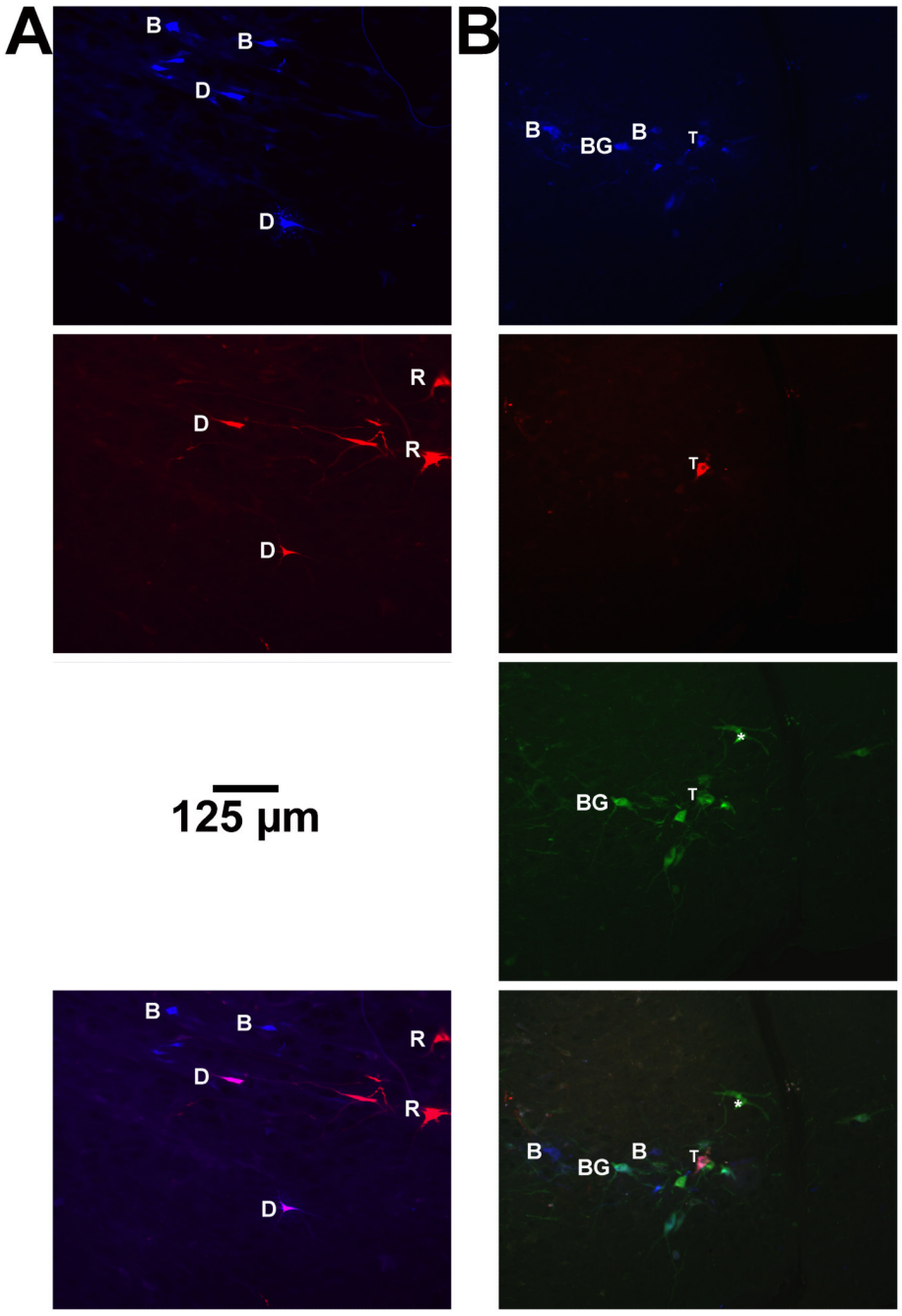

Figure 5.

Photomicrographs illustrating RVLM neurons that were labeled by injections of Fast Blue into T_4 and Fluoro-Ruby in T_{10}, in sections that either were not ***(A)*** or were ***(B)*** processed to visualize tyrosine hydroxylase (TH). ***A*** is from a section through the RVLM of animal C48, whereas ***B*** is from animal C13. In each panel, the top row shows Fast Blue labeling, the second row shows Fluoro-Ruby labeling, the third row shows immunofluorescence for TH ***(B only)*** and the fourth row shows all fluorophors. Examples of neurons that were selectively labeled by Fast Blue (B), Fluoro-Ruby (R), or which were immunopositive for TH (*) are indicated, as well as neurons that were double-labeled for both Fast Blue and

Fluoro-Ruby (D) and Fast Blue and TH (BG). A cell that was triple-labeled for Fast Blue, Fluoro-Ruby, and TH is indicated by (T).

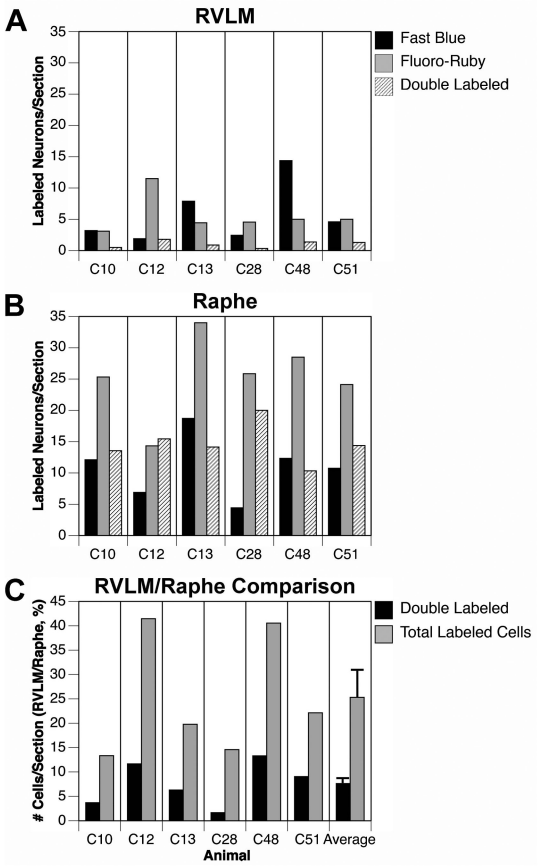

Figure 6.

The number of tracer-labeled RVLM neurons in each animal, and comparisons with labeling in the caudal raphe nuclei of the same animals. ***A:*** average number of labeled neurons per section in the RVLM. ***B:*** average number of labeled neurons per section in the medullary raphe nuclei (raphe pallidus and obscurus combined). ***C:*** comparison of the total number of labeled cells and the number of double-labeled cells/section in the RVLM and caudal medullary raphe nuclei. Values are shown as the number of cells per section in the RVLM as a fraction of the number of cells per section in the raphe nuclei. The right column shows the average and standard error of values for all animals.

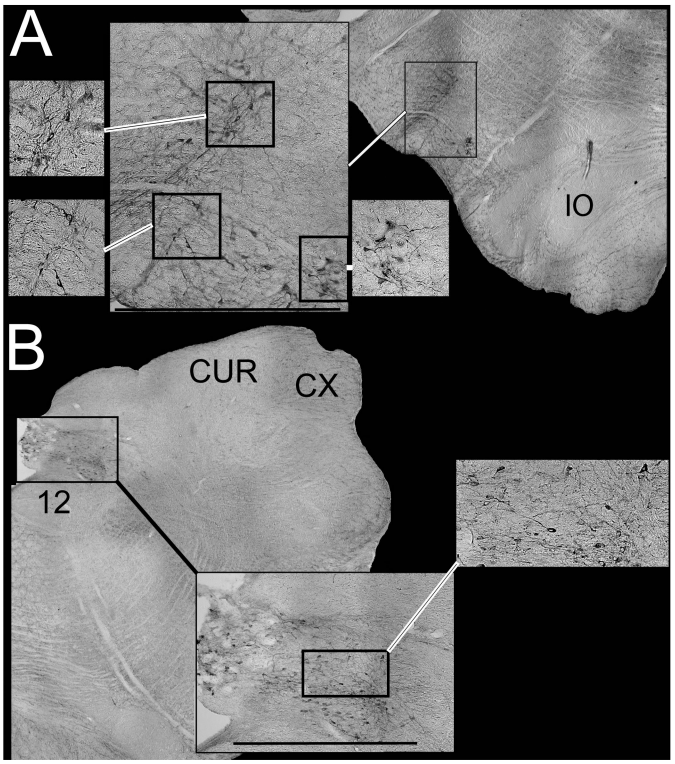

Figure 7.
Photomicrographs of RVLM ***(A)*** and NTS ***(B)*** neurons that were immunopositive for TH. Cell locations are indicated on photomontages of low-power micrographs. Calibration bars on the larger inset figures designate 1 mm. Abbreviations: 12, hypoglossal nucleus; CUR, rostral cuneate nucleus; CX, external cuneate nucleus; IO, inferior olive.

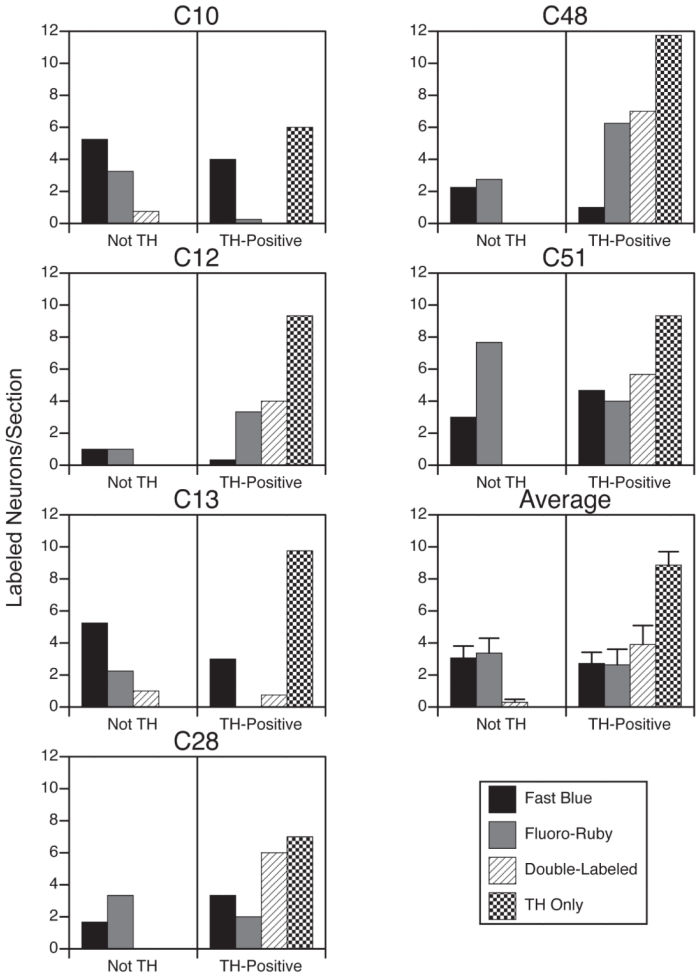

Figure 8.

Average number of tracer-labeled neurons per section within the cluster of RVLM neurons that were immunopositive for tyrosine hydroxylase (TH). Each animal is represented in a separate panel. Counts were divided based on whether neurons in the cluster were TH-negative (Not TH) or TH-positive. The average number of TH-immmunopositive neurons per section that was not labeled by tracers is also indicated. The bottom panel in the right column shows average values for all animals; error bars designate one standard error.

Table 1

Injection site volumes in each experiment. Three tracer injections of this volume, spaced 1 mm apart, were placed in the target segments.

Experiment	Volume of Each Fast Blue Injection in T_4	Volume of Each Fluoro-Ruby Injection in T_{10}
C102	----	200 μL
C101	100 μL	----
C12	250 μL	250 μL
C11	250 μl	200 μL
C10	250 μL	250 μL
C13	250 μL	250 μL
C24	250 μL	250 μL
C28	250 μL	250 μL (2 injections) 300 μL (1 injection)
C51	500 μL	500 μL
C47	150 μL	150 μL
C49	500 μL	500 μL
C48	150 μL	150 μL

Table 2

Average coordinates (mean ± SEM) of RVLM neurons labeled selectively by Fast Blue injected into T_4, Fluoro-Ruby injected into T_{10}, or which were double-labeled by both tracers. Values for the left and right sides, and the totals for both sides, are indicated separately.

Tracer	Side	n	Distance from Rostral Tip of Inferior Olivary Nucleus (mm)	Distance from Ventral Surface of the Brainstem (mm)	Distance Lateral to the Midline (mm)
Fast Blue	*Left*	148	0.8 ± 0.05	0.6 ± 0.02	3.5 ± 0.05
	Right	215	0.8 ± 0.04	0.5 ± 0.02	3.5 ± 0.04
	Total	363	0.8 ± 0.03	0.6 ± 0.03	3.5 ± 0.03
Fluoro-Ruby	*Left*	127	0.9 ± 0.05	0.6 ± 0.03	3.4 ± 0.05
	Right	190	0.8 ± 0.05	0.5 ± 0.02	3.3 ± 0.04
	Total	317	0.9 ± 0.04	0.5 ± 0.01	3.4 ± 0.03
Double-Labeled	*Left*	29	0.9 ± 0.1	0.7 ± 0.04	3.6 ± 0.08
	Right	29	0.7 ± 0.1	0.6 ± 0.04	3.4 ± 0.1
	Total	58	0.8 ± 0.07	0.5 ± 0.03	3.5 ± 0.07